# EXPERIMENTAL METHODS FOR DETERMINING STRESS INTENSITY FACTORS

**P. S. Theocaris**

*Department of Theoretical and Applied Mechanics, The National Technical University of Athens, 5 Heroes of Polytechnion Avenue, GR-157 73 Athens, Greece*

ABSTRACT

The lecture reviews, in broad terms, the development of experimental fracture mechanics during the last two decades. Optical standard techniques for the experimental determination of K-factors are surveyed and recent developments of the methods are presented. Emphasis is given to the widely utilized methods of photoelasticity and caustics.

KEYWORDS

Linear elastic fracture mechanics; stress intensity factors; Muskhelishvili's and Westergaard's stress functions; dynamic crack propagation; isochromatics; isopachics; caustics; photoelasticity; moiré; interferometry.

## INTRODUCTION

Experimental fracture mechanics is of paramount importance to the practitioner, because it provides him with an immediate solution of problems concerning concentrations of stresses and strains in cracked or notched elements of structures and machines, which cannot be otherwise directly observed, and which are usually beyond the reach of calculation. On the other hand, the theoretician, in contact with the experimental developments, gets more intuition and ideas, which provide a basis for further theoretical analysis. The lack of many quantitative theories, e.g. for dynamic crack problems and the general demand for checking the analytical studies create the need of more and more sophisticated experiments in the area of fracture mechanics. This is one of the basic necessities in fracture mechanics and it is hopeful that, at the present state, the experimental studies all over the world are directed toward this target.

Experiments on fracture are executed for diverse purposes: testing of criteria predicting material failure, Charpy values, crack opening displacement (COD), etc. Here, we are restricted either to the formulation of fracture-mechanics theories, or to engineering specifications of materials. The stress field produced in an elastic cracked plate has a universal

spatial dependence and the only quantity, which varies from one specific case of loading-conditions and geometry to another is a scalar, the so-called *stress intensity factor* K. From the practical point of view, the stress singularity at the crack tip can be characterized by the K-factor, and the critical load required to start a pre-existing crack or notch in a plate can be predicted, if the fracture toughness, expressed by $K_c$, of the material is known. The usefulness and the attractiveness of the experimental methods presented in this lecture are due to the fact that they provide a direct measure of the SIFs, without any consideration of field quantities or boundary conditions.

The state of the art in the experimental methods for the determination of stress intensity factors (SIFs) is reviewed and recent progress exclusively in optical techniques is outlined. It should be understood that it would be impossible to adequately treat all the details of the important developments in the domain of experimental fracture mechanics in this lecture. Therefore, descriptions of the various experimental techniques will be brief; only their essential features and some of characteristic applications to practical problems will be critically presented. It is the author's hope that the readers of this lecture, will be able to identify particular techniques, which perform their claims, and refer back to the original papers for further study.

## THEORETICAL PRELIMINARIES

For a homogeneous isotropic or anisotropic planar body, containing a straight crack in the Oxz-plane, three fundamental stress fields are associated with the three modes of crack surface displacements (Irwin, 1958; Paris and Sih, 1965). Mode-I displacements occur when the crack faces separate normally (in the Oy-direction) to one another. For mode-II, the displacements of the crack faces are normal to the crack front (in the Ox-direction) and in the crack plane. In mode-III, the displacements of the crack faces are parallel to the crack front (in the Oz-direction) and in the crack plane. In the theory of two-dimensional isotropic elasticity, the stresses and displacements may be expressed in terms of two complex functions $\Phi(z)$ and $\Psi(z)$ of the variable $z=x+iy$ (Kolosoff, 1909; Muskhelishvili, 1953). These complex potentials are related to the Airy stress function F by

$$F = \mathrm{Re}[\bar{z}\Phi(z)+\Psi(z)] \tag{1}$$

Special cases of the Kolosoff formulae are given by Westergaard, 1939, and they were widely utilized by the practitioners and experimentalists in fracture mechanics for many years. Analogous relations may be derived for the dynamic crack propagation (Radok, 1956).
Similar to dynamic relations may be also derived for the case of a stationary crack traversing an anisotropic plate (Sih and co-workers, 1965).
Following Irwin's analysis (1957) and factoring out the K-factors from the series expansions of the complex potentials, the stress-components take the following form for an infinite plate with an internal stationary crack of length $2\alpha$, inclined at angle $\beta$ with the imaginary axis, and loadings $\sigma_{\infty y}, \sigma_{\infty x}=k\sigma_{\infty y}$ at infinity (Theocaris, 1977; Theocaris and Spyropoulos, 1983).

$$\sigma_x = \frac{K_I}{2(\pi\alpha)^{\frac{1}{2}}}\left\{\left(\frac{r}{2\alpha}\right)^{-\frac{1}{2}}\cos\left(\frac{\vartheta}{2}\right)\left[1-\sin\left(\frac{\vartheta}{2}\right)\sin\left(\frac{3\vartheta}{2}\right)\right] + \frac{3}{2}\left(\frac{r}{2\alpha}\right)^{\frac{1}{2}}\cos\left(\frac{\vartheta}{2}\right)\right.$$



$$\left[1+\sin^2\left(\frac{\vartheta}{2}\right)\right] + \sum_{n=1}^{\infty}\left(\frac{r}{2\alpha}\right)^{n+\frac{1}{2}}\frac{2n+3}{2n+2}(-1)^n\frac{1.3\ldots(2n-1)}{2.4\ldots(2n)}\left[\cos\left(n+\frac{1}{2}\right)\vartheta\right.$$

$$\left.\left.-\left(n+\frac{1}{2}\right)\sin\vartheta\sin\left(n-\frac{1}{2}\right)\vartheta\right]\right\} + \sigma_{\infty y}(1-k)\cos 2\beta + \frac{K_{II}}{2(\pi\alpha)^{\frac{1}{2}}}$$

$$\left\{-\left(\frac{r}{2\alpha}\right)^{\frac{1}{2}}\sin\left(\frac{\vartheta}{2}\right)\left[2+\cos\left(\frac{\vartheta}{2}\right)\cos\left(\frac{3\vartheta}{2}\right)\right] + \frac{3}{2}\left(\frac{r}{2\alpha}\right)^{\frac{1}{2}}\sin\left(\frac{\vartheta}{2}\right)\left[2+\cos^2\left(\frac{\vartheta}{2}\right)\right] + \right.$$

$$+\sum_{n=1}^{\infty}\left(\frac{r}{2\alpha}\right)^{n+\frac{1}{2}}\frac{2n+3}{2n+2}(-1)^n\frac{1.3\ldots(2n-1)}{2.4\ldots(2n)}\left[2\sin\left(n+\frac{1}{2}\right)\vartheta + \right.$$

$$\left.\left.+\left(n+\frac{1}{2}\right)\sin\vartheta\cos\left(n-\frac{1}{2}\right)\vartheta\right]\right\}$$

$$\sigma_y = \frac{K_I}{2(\pi\alpha)^{\frac{1}{2}}}\left\{\left(\frac{r}{2\alpha}\right)^{-\frac{1}{2}}\cos\left(\frac{\vartheta}{2}\right)\left[1+\sin\left(\frac{\vartheta}{2}\right)\sin\left(\frac{3\vartheta}{2}\right)\right] + \frac{3}{2}\left(\frac{r}{2\alpha}\right)^{\frac{1}{2}}\cos^3\left(\frac{\vartheta}{2}\right) + \right.$$

$$+\sum_{n=1}^{\infty}\left(\frac{r}{2\alpha}\right)^{n+\frac{1}{2}}\frac{2n+3}{2n+2}(-1)^n\frac{1.3\ldots(2n-1)}{2.4\ldots(2n)}\left[\left(n+\frac{1}{2}\right)\sin\vartheta\sin\left(n-\frac{1}{2}\right)\vartheta + \right.$$

$$\left.\left.+\cos\left(n+\frac{1}{2}\right)\vartheta\right]\right\} + \frac{K_{II}}{2(\pi\alpha)^{\frac{1}{2}}}\left\{\left(\frac{r}{2\alpha}\right)^{-\frac{1}{2}}\sin\left(\frac{\vartheta}{2}\right)\cos\left(\frac{\vartheta}{2}\right)\cos\left(\frac{3\vartheta}{2}\right) - \right.$$

$$-\frac{3}{2}\left(\frac{r}{2\alpha}\right)^{\frac{1}{2}}\sin\left(\frac{\vartheta}{2}\right)\cos^2\left(\frac{\vartheta}{2}\right) - \sum_{n=1}^{\infty}\left(\frac{r}{2\alpha}\right)^{n+\frac{1}{2}}\frac{2n+3}{2n+2}(-1)^n\frac{1.3\ldots(2n-1)}{2.4\ldots(2n)}$$

$$\left.\left(n+\frac{1}{2}\right)\sin\vartheta\cos\left(n-\frac{1}{2}\right)\vartheta\right\}$$

$$\tau_{xy} = \frac{K_I}{2(\pi\alpha)^{\frac{1}{2}}}\left\{\left(\frac{r}{2\alpha}\right)^{-\frac{1}{2}}\sin\left(\frac{\vartheta}{2}\right)\cos\left(\frac{\vartheta}{2}\right)\cos\left(\frac{3\vartheta}{2}\right) - \frac{3}{4}\left(\frac{r}{2\alpha}\right)^{\frac{1}{2}}\sin\left(\frac{\vartheta}{2}\right)\cos\left(\frac{\vartheta}{2}\right) - \right.$$

$$\left.-\sum_{n=1}^{\infty}\left(\frac{r}{2\alpha}\right)^{n+\frac{1}{2}}\frac{2n+3}{2n+2}(-1)^n\frac{1.3\ldots(2n-1)}{2.4\ldots(2n)}\sin\vartheta\cos\left(n-\frac{1}{2}\right)\vartheta\right\} +$$

$$+\frac{K_{II}}{2(\pi\alpha)^{\frac{1}{2}}}\left\{\left(\frac{r}{2\alpha}\right)^{-\frac{1}{2}}\cos\left(\frac{\vartheta}{2}\right)\left[1-\sin\left(\frac{\vartheta}{2}\right)\sin\left(\frac{3\vartheta}{2}\right)\right] + \frac{3}{2}\left(\frac{r}{2\alpha}\right)^{\frac{1}{2}}\cos\left(\frac{\vartheta}{2}\right)\right.$$

$$\left[1+\sin^2\left(\frac{\vartheta}{2}\right)\right] + \sum_{n=1}^{\infty}\left(\frac{r}{2\alpha}\right)^{n+\frac{1}{2}} \frac{2n+3}{2n+2}(-1)^n \frac{1.3\ldots(2n-1)}{2.4\ldots(2n)}$$

$$\left.\left[\cos\left(n+\frac{1}{2}\right)\vartheta - \left(n+\frac{1}{2}\right)\sin\vartheta\sin\left(n-\frac{1}{2}\right)\vartheta\right]\right\} \qquad (2)$$

Generally, in all stress fields around cracks a constant term $\sigma_{ox}$ will be arised, which is similar to $\sigma_{\infty y}(1-k)\cos 2\beta$ in the above relations. For mixed mode propagating cracks, the Sneddon-Radok equations give

$$\sigma_x = \frac{K_I B_I}{(2\pi)^{\frac{1}{2}}}\left[(1+2\beta_1^2-\beta_2^2)\frac{\cos(\vartheta_1/2)}{r_1^{\frac{1}{2}}} - \frac{4\beta_1\beta_2}{(1+\beta_2^2)}\frac{\cos(\vartheta_2/2)}{r_2^{\frac{1}{2}}}\right] +$$

$$+ \frac{K_{II} B_{II}}{(2\pi)^{\frac{1}{2}}}\left[-(1+2\beta_1^2-\beta_2^2)\frac{\sin(\vartheta_1/2)}{r_1^{\frac{1}{2}}} + (1+\beta_2^2)\frac{\sin(\vartheta_2/2)}{r_2^{\frac{1}{2}}}\right] + \text{(other terms)}$$

$$\sigma_y = \frac{K_I B_I}{(2\pi)^{\frac{1}{2}}}\left[-(1+\beta_2^2)\frac{\cos(\vartheta_1/2)}{r_1^{\frac{1}{2}}} + \frac{4\beta_1\beta_2}{(1+\beta_2^2)}\frac{\cos(\vartheta_2/2)}{r_2^{\frac{1}{2}}}\right] +$$

$$+ \frac{K_{II} B_{II}}{(2\pi)^{\frac{1}{2}}}\left[(1+\beta_2^2)\frac{\sin(\vartheta_1/2)}{r_1^{\frac{1}{2}}} - (1+\beta_2^2)\frac{\sin(\vartheta_2/2)}{r_2^{\frac{1}{2}}}\right] + \text{(other terms)}$$

$$\tau_{xy} = \frac{K_I B_I}{(2\pi)^{\frac{1}{2}}}\left[2\beta_1\frac{\sin(\vartheta_1/2)}{r_1^{\frac{1}{2}}} - 2\beta_1\frac{\sin(\vartheta_2/2)}{r_2^{\frac{1}{2}}}\right] +$$

$$+ \frac{K_{II} B_{II}}{(2\pi)^{\frac{1}{2}}}\left[2\beta_1\frac{\cos(\vartheta_1/2)}{r_1^{\frac{1}{2}}} - \frac{(1+\beta_2^2)}{2\beta_2}\frac{\cos(\vartheta_2/2)}{r_2^{\frac{1}{2}}}\right] + \text{(other terms)} \qquad (3)$$

where $$B_I = \frac{1+\beta_2^2}{4\beta_1\beta_2-(1+\beta_2^2)^2}, \quad B_{II} = \frac{2\beta_2}{4\beta_1\beta_2-(1+\beta_2^2)^2} \qquad (4)$$

and $z_j = x+i\beta_j y = r_j e^{i\vartheta_j}$ $(j=1,2)$, where $\beta_j^2 = 1-\upsilon^2/c_j^2$, $\upsilon$ being the crack velocity and $c_j$ being the longitudinal (j=1)- and shear (j=2)-wave velocities.
It may be noticed that the parts of the non-singular terms in Eqs.(2), which are independent of the r- and $\vartheta$-coordinates, are different for other boundary conditions. Particularly, the independent term of r- and $\vartheta$-coordinates, mostly designated as $\sigma_{ox}$, in the $\sigma_x$-stress expression was considerably studied (Liebowitz et al., 1978). However, it will be shown that this term does not influence the size and the shape of caustics, whereas it plays a significant role in the interpretation of SIFs from photoelastic experiments. Irwin and co-workers (1979) established that, for SEN-specimens (Single Edge Notched) and MCT-wedge-loaded-specimens (Modified Compact Tension), $\sigma_{ox}$ is relatively small, for MCT-pin-loaded-specimens, $\sigma_{ox}$ is medium and for DCB-specimens (Double Cantilever Beam), $\sigma_{ox}$ is large, with respect to the remaining part in the $\sigma_x$-expression.
Rather comprehensive collections of SIFs are contained in Sih (1962), and Paris and Sih (1965). Catalogs of values of SIFs for several problems have been published by Cartwright and Rooke (1974), Tada, Paris and Irwin (1973) and Sih (1973). Most of the solutions included in these treatises have been derived analytically, as well as numerically.



Whereas in the early days of fracture mechanics studies, experimental techniques were based on strain-gage measurements, in this review we shall not present any application of this experimental technique, restricting ourselves to the more potential optical methods. For the same reasons acoustic-emission techniques will be avoided.

## MOIRÉ METHOD

The moiré effect is an optical phenomenon observed when two arrays of lines or dots are superimposed (Lord Rayleigh, 1874). If the arrays consist of opaque parallel lines, which are not identical in spacing or orientation, then moiré fringes are formed as the lines of one array alternately fall on, or between, the lines of the other array (Theocaris, 1969). The method based on the moiré effect was widely utilized in the analysis of deformation of solids. The basic elements of the technique is as follows (Theocaris, 1969; Durelli and Parks, 1970): A *model* grating is associated with the surface deformations of a specimen, acting as a *reference element* of the changes of the surface from the initial to deformed state. In order to determine the changes in the geometry of the *model grating*, a second grating, the *reference grating* is introduced. Then, a moiré pattern is formed on the image plane of the observation system. Moiré fringes are loci of points, having the same component of displacement in a direction perpendicular to the grid lines of the undistorted grating. The complete moiré pattern can thus be visualized as a displacement surface, where the height of a point on the surface above a reference plane represents the displacement of the point in the perpendicular direction to the reference-grating lines. This approximate interpretation can be used, without serious error, as long as the deformations are small. Three moiré patterns, oriented at different angles with respect to one another, can be used to find three normal components of strain at any point in the field. The well-known strain-rosette formula can then be applied to determine the principal strains and their directions. Therefore, a moiré pattern is equivalent to an infinite number of strain-gage rosettes on the surface of the specimen. The moiré fringe method determines the displacement field directly, and therefore the appropriate stress function can be determined by fitting this function to the experimentally determined displacement field in the vicinity of a stationary or running crack tip. A series expansion of the complex potentials leads to expressions for the $u_x$- and $u_y$-displacements, analogous to Eqs.(2). For instance, the mode-I static displacement field can be expressed as

$$u_x = \frac{K_I}{G}\left(\frac{r}{2\pi}\right)^{\frac{1}{2}}\cos\left(\frac{\vartheta}{2}\right)\left[\frac{1-\nu}{1+\nu} + \sin^2\left(\frac{\vartheta}{2}\right)\right] + \text{(other terms)}$$

$$u_y = \frac{K_I}{G}\left(\frac{r}{2\pi}\right)^{\frac{1}{2}}\sin\left(\frac{\vartheta}{2}\right)\left[\frac{2}{1+\nu} - \cos^2\left(\frac{\vartheta}{2}\right)\right] + \text{(other terms)} \qquad (5)$$

Taking measurements from a number of points in the close vicinity of the crack tip, the K-factors may be determined from Eqs.(5), or analogous relations. The technique must be applied with care to the dynamic crack propagation in strain-rate sensitive materials, where the shear modulus G changes allover the specimen, throughout the period of propagation. The

moiré method in fracture mechanics was succesfully applied to several crack problems by Kobayashi and co-workers (1965; 1967; 1969). The pattern around a static crack in Fig.1 is taken from an unpublished work of the present author.

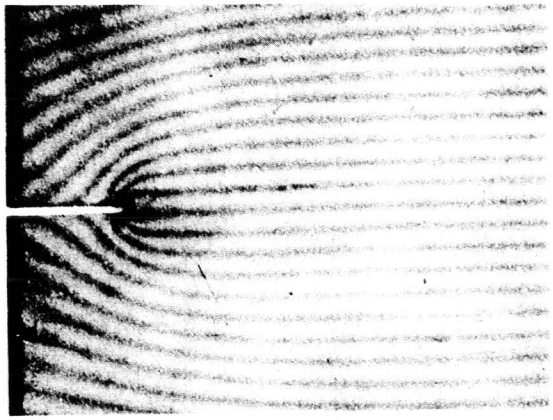

Fig. 1. Photograph of moiré fringes around an edge crack.

In spite of an obvious lack of sensitivity, the moiré method is really a valuable method for the determination of the amplitude of the singularity $K_\sigma$, (Hutchinson 1968) in the presence of small-scale yielding around a crack tip. However, experiments performed by Liu et al. (1970) in cracked plates made of an aluminium alloy, shows disagreement between the $r^{-(1/1+n)}$ theoretical distribution of strains and the $r^{-1/2}$ experimental distribution around the plastically deformed crack tip.

## INTERFEROMETRY

Interferometry is a powerful tool for measuring strains, deformations and deflections and its high accuracy makes it capable for applying it to experimental fracture mechanics. This method can measure absolute variations of the optical path in the two principal directions (Favre, 1929). Variations of the Favre principle were reviewed by Theocaris (1969). Interferometric measurements were also used to obtain isopachic patterns in thin specimens under generalized plane-stress (Theocaris, 1963). Post (1953) has introduced interferometry in fracture mechanics and Oppel and Hill (1964) initiated the use of interferometry as a technique for qualitative plastic-zone studies at the roots of cracks and notches.
For any point in an elastic plane-stress plate, it is valid that

$$\Delta d = - \frac{\nu d}{E} (\sigma_1+\sigma_2) \qquad (6)$$

where d is the thickness of the unloaded specimen, $\Delta d$ the variation of thickness under load and $\sigma_1, \sigma_2$ the principal stresses.
Thus, a precise measurement of the change of thickness caused by loading allows the accurate evaluation of the sum of the principal stresses in the plane-stress system. If light rays are incident upon a transparent plate, a small portion of the light is reflected back from each surface. For typical polymers resembling glass, for which the refractive index may be taken approximately equal to n=1.5, it can be deduced (Born and Wolf, 1970) that almost equal intensities of the order of 4% are reflected from the front and rear faces, and the multiple reflections are relatively insignificant. Thus, the first reflections from the front and rear faces, being of equal amplitude, can readily, in the case of sufficient optical coherence, interfere to form high-contrast interference patterns (Haidinger fringes). With light travelling at a constant velocity in the material, the relative phase is a function of the optical path difference. The loci of points satisfying the well-known interference relation form dark fringes, representing contour lines of constant plate thickness. Photographs are taken of the model in the loaded and unloaded state. The fringe shift $\Delta n$, caused by the loading, may be counted for any point, and the $(\sigma_1+\sigma_2)$-sum of stresses can be readily and accurately derived.
Fig.2 shows the pattern of isopachics around an internal transverse mode-I crack (Theocaris and Spyropoulos, 1982).

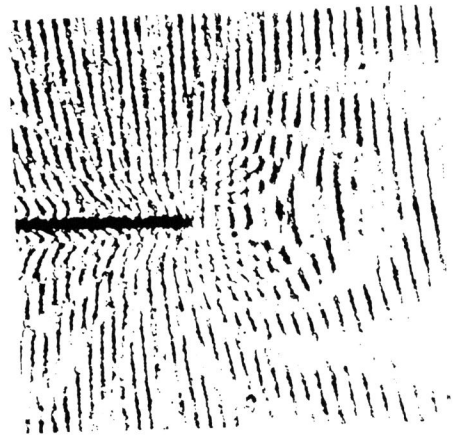

Fig. 2. Experimentally obtained isopachic fringe pattern for mode-I, deformation.

The only disadvantage of the method, as it is presented above, is the necessity of the initial uniformity of thickness of the model, to avoid excessively high fringe-densities.
The last restriction can be avoided by using holographic interferometry. *Holography*, or *wave-front reconstruction*, is a method of storing information concerning the three-dimensional nature of an object (Gabor, 1948; Leith and Upatnieks, 1963;1964). In holography, standing waves are formed by the interference of two coherent-light beams in the plane of a high-resolution photographic plate. The developed plate (*hologram*) is a diffraction grating, which has the important property of reconstructing the *object beam*, when it is placed exactly at its initial position and illuminated by the reference beam under identical conditions of geometry of the experimental set-up.
First, a reference hologram is taken of the model in its unloaded state. The load is then applied and a second hologram was recorded on the same plate. The loading causes a change in the optical thickness of the model and, hence, a slightly different image than the reference image. In the reconstructing procedure of the hologram, these two images interfere, resulting in an isopachic fringe pattern. A geometric interpretation of holography, based on the theory of moiré, was given by Theocaris (1971).

The important advantage of the holographic interferometry is that only the change in the optical thickness, that occurs between the two exposures is recorded. Therefore, there is no restriction for perfect flatness or parallel faces (Fourney, 1968). Fig.3 shows holographic interferograms of crack tip region in a Polymethyl-methacrylate (PMMA) specimen at 96 percent of the fracture load, as recorded by Dudderar and O'Regan (1971).

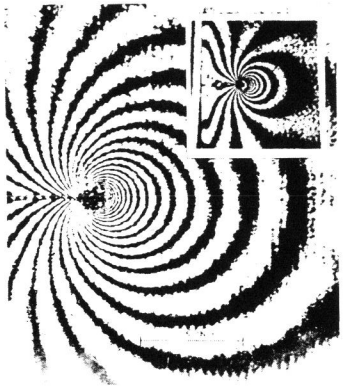

Fig. 3. Near- and far-field holographic interferograms of crack region in a PMMA specimen (courtesy of Dr. T.D. Dudderar).

In transmission interferometry the intensity equation becomes equal to zero and yields dark fringes at loci where the $\varepsilon_z$-strain is expressed by

$$\varepsilon_z = \frac{-\lambda(2N+1)}{2(n-1)d} \qquad (7)$$

where $\lambda$ is the optical wave-length and N is the fringe order.
On the other hand, from the elastic solution of the problem of a cracked plate under mode-I deformation the singular part of the $\varepsilon_z$-strain is expressed by

$$\varepsilon_z = -\frac{2\nu K_I \cos(\vartheta/2)}{E(2\pi r)^{\frac{1}{2}}} \qquad (8)$$

Eqs.(7) and (8), give the stress intensity factor in terms of material- and experimental-arrangement parameters, the fringe order N and the location of the point of measurement.

Since the interpretation of the optical pattern near the crack tip is difficult, due to various perturbations,such as the steep variation of the stress field, which indicate a steep variation of the isopachics, the triaxiality of the stress field, the nonlinear variation of the refractive index, etc., the region far from the crack tip is the only convenient region for measurements. Therefore, by ignoring terms, which affect the isopachic fringe patterns, inaccurate results are obtained in evaluating the SIFs. The following general method (Theocaris and Spyropoulos, 1982) for the determination of SIFs using interferometry is briefly discussed: The first invariant I of the normal stresses is taken from Eq.(2) in a series expansion form. Measuring now the instantaneous crack length $2\alpha$ and having the experimental value of the invariantat $I=Nf_p/d$, where $f_p$ is the isopachic-fringe constant, the expression of the invariant I may be written as

$$I = BK_I + CK_{II} + X \qquad (9)$$

where B and C are functions of the coordinates of selected points and the crack length and

$$X = \sigma_\infty(1-k)\cos 2\beta \qquad (10)$$

Eq.(10), applied to three points arbitrarily selected from an isopachic fringe pattern, gives a set of three linear equations with three unknowns, the $K_I$- and $K_{II}$-stress intensity factors and the quantity X, which can be readily evaluated when this system is solved. The isopachic method was also introduced in the problem of fast running cracks by using a pulsed ruby laser and the high-speed photography technique (Holloway et al., 1978). Rossmanith (1979) inserted a dynamic correction, in the interpretation of Holloway's experiments and derived the dynamic stress intensity factor, using the singular expressions with the addition of the constant $\sigma_{ox}$-term only.

In conclusion, interferometry is a valuable method for the experimental determination of SIFs which, nevertheless has not been applied widely by experimenters, because, mainly, it requires complicated apparatuses and many measurements, when high accuracy is desired.

## PHOTOELASTIC METHOD

Photoelastic measurements interrelate the relative retardation with certain stress- or strain-components. The method can be sensitive and precise and is self-sufficient for the determination of the magnitude and directions of maximum shear stresses. The photoelastic method was first applied to fracture mechanics problems by Post (1953) for stationary cracks, and Wells and Post (1958) for running cracks. In the well-known discussion of the above-mentioned paper by Wells and Post, Irwin (1958) suggested a technique for the determination of $K_I$-factor, exploiting photoelastic fringes. Since these early studies, much time has been devoted to develop new methods, or refinements of the original ones, for evaluating SIFs, either in static, or in dynamic cracks.
Irwin's *two-parameter method* retains only the singular and the constant term and expresses the maximum shear stress $\tau_m$, given by the isochromatics in a photoelastic stress pattern, in terms of the cartesian components of stresses. Definition of the polar angle $\vartheta$,for which a maximum for the $\tau_m$-stress exists for a single fringe loop of the photoelastic pattern,allows the evaluation of $K_I$ and $\sigma_{ox}$-stress.
Etheridge and Dally (1977) have pointed out, in a review article, that the two-parameter methods are applicable for determining $K_I$-factors in the range $73^o<\vartheta_m<139^o$, provided $r_m/\alpha<0.03$, where $r_m$ is the apogee distance and $\vartheta_m$ is the fringe loop tilt. If no measurement errors are made in $r_m$ or $\vartheta_m$, the preceding methods predict $K_I$ with ±5 percent accuracy.

*Three-parameter methods* ($r^{-\frac{1}{2}}$,$r^{\frac{1}{2}}$-and $\sigma_{ox}$-terms included in the series expansion), proposed by Ioakimidis and Theocaris (1978), and Etheridge and Dally (1978), have improved considerably the accuracy of SIF-evaluation and allowed measurements outside the close vicinity of the crack tip for mode-I deformation. The first technique was based on properties of complex functions and simple geometrical relations and made use of the relation $\sigma_{ox}=\pm 2\tau_m$ for y=0 and the polar expression for $K_I$ for an angle $\vartheta$,given by

$$\tau_m|\cos\vartheta| = \left|\frac{\sigma_{ox}}{2}\cos\left(\frac{3\vartheta}{2}\right)\right| \qquad (11)$$

The second one was based on measurements of $r_m$ and $\vartheta_m$ from any two independent fringe loops and results to a cubic equation for the $r^{\frac{1}{2}}$-parameter which, when solved, gives the $K_I$- and $\sigma_{ox}$-values.

All preceding methods necessitate measurements from the close vicinity of the crack-tip, because they use terms only up to $r^{\frac{1}{2}}$, which is the lowest-order non-singular term in the series expansion. On the other hand, there is a number of reasons, which dictate the obligation to take experimental data in regions relatively far from the crack tip: a) The geometry of the artificial notches, which are often used to simulate the real cracks, influences greatly the near to the bottom of the notch stress field. This effect has extensively been studied by Smith and co-workers (1972;1974), who found the influence of the end-notch geometry on the stress intensity factors

for various notch configurations. They established that the difference between the stress fields existing at the tip of a real crack and at the end of a notch, is considerable in the close vicinity of these regions. Creager and Paris (1967) gave also the expressions of stresses for a slit with radius $\rho$ at the root of the notch under mode-I deformation, by adding in Eqs.(2) a corrective term to the expressions of the stress components. After this correction it is seen that, while the photoelastic measurements are related to the difference of principal stresses, and therefore to all Cartesian components of stresses, are dependent on the radius $\rho$ of the root, measurements based on caustics or interferometry, which depend only on the sum of principal stresses, are independent of $\rho$. b) The high-stress concentration at the vicinity of the crack tip results in an enhanced isochromatic-fringe density, so that the order of the isochromes in this region may exceed the linear limit in the stress-fringe order curve of the material. c) The high strain gradients near the crack tip create a region of three-dimensional stresses in specimens of finite thickness and therefore deviations from the two-dimensional theory. d) Non-linearity effects, as well as formation of voids and crazes in the crack tip zone.
For all the above and other reasons, although the idea of using the photoelastic method of stress analysis to the solution of crack problems seems to be attractive, many difficulties are encountered during the application of the method, especially in real crack problems, where neither the form of the crack, nor the near to the crack stress fields take an idealized form. Indeed, Fig.4, taken from Dally (1979), shows a photoelastic experiment with a branched propagating crack, where any measurement at the close vicinity of the crack tips seems to be impossible.

Fig. 4. Isochromatic-fringe pattern representing crack propagation after branching (courtesy of Prof. J.W. Dally).

Two different approaches (Theocaris and Gdoutos, 1978, Theocaris and Spyropoulos, 1983) have been employed to overcome the already mentioned difficulties, by taking measurements outside the undesirable crack tip-region. The first one is based on a comparison between the far- and the near-to-the-crack tip stress fields and the use of suitable extrapolation laws for the determination of the near stress-field characteristic parameters, by gathering data from the far-stress field. The second one, making use of the series expansion-relations, i.e. Eq.(2), results in a system of three non-linear equations of the three unknowns $K_I$, $K_{II}$ and $\sigma_{ox}$. This system can be solved with the *Newton-Raphson* method. Three measurements of r- and $\vartheta$-coordinates in one fringe loop are required. A predetermined accuracy with respect to the external load is introduced, in order that no amount of terms greater than the predetermined accuracy is added. Fig. 5 (Theocaris and Spyropoulos, 1983), shows a comparison between analytically generated isochromatic fringes when higher order terms are considered in Eq.(2). Only the four-term (dotted) lines approximate satisfactorily the seven-term (continuous) isochromatic lines.

Three-dimensional crack problems treated by photoelastic techniques during the last decade were executed mainly by Smith and his associates. Reviews of this work one can find in Smith



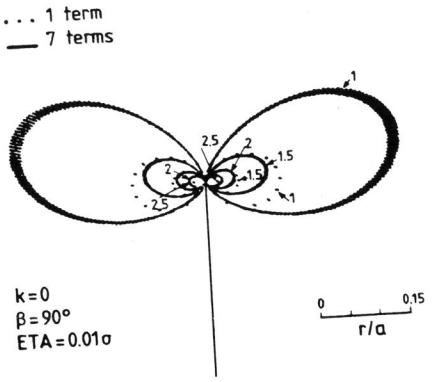


Fig. 5. Pattern of isochromes in an infinite plate with an internal transverse crack submitted to mode-I deformation as plotted by computer.

(1975;1981) and thus it is not considered necessary to give here details of these studies. However, if one considers the difficulties in solving analytically crack-problems in three dimensions, and especially in part-through cracks, where, besides the three-dimensionality of the problem, its asymmetry in loading and geometry is added, the solutions by Smith, based on classical photoelasticity, constitutes actually, perhaps, the only secure information, concerning this important problem. In three-dimensional through-crack problems also, experiments were conducted by Villarreal and Sih (1981) to confirm the Hartranft-Sih theory (1968;1970) by the use again of the frozen-stress technique.

Since the pioneering work of Wells and Post (1958), photoelasticity was employed in numerous dynamic studies of fracture. Among others, Kobayashi and co-workers (1970; 1971;1977;1978;1981) and Dally and co-workers (1977;1978;1979) developed techniques to interpret dynamic isochromatic fringes, or applied dynamic photoelasticity in special problems. The recording systems involve a Cranz-Schardin multiple-spark, high-speed camera (Wells and Post, 1958; Riley and Dally, 1969). Up to the seventies, a static analysis was employed to evaluate mode-I SIFs from a dynamic experiment. The first attempt to analyze fringes associated with dynamic cracks, utilizing a dynamical crack propagation theory (Yoffé, 1951; Radok, 1956), is due to Bradley and Kobayashi (1971). Rossmanith and Irwin (1979), utilizing dynamic expressions for a mode-I crack, moving under constant velocity, gave, in the form of correction factors, the $K_I^{dyn}$-stress intensity (Dally, 1979). Later on, Kobayashi and Ramulu (1981), using the same dynamic solution, extended the preceding method to mixed-mode crack propagation. They established that relatively small differences exist between the stress distributions around static and dynamic cracks. Very recently also, Kobayashi (1982) extended his previous analysis to the case of small plastic zones around the opening dynamic cracks, using the Dugdale strip-yield-zone model (Kanninen, 1968).

## THE METHOD OF CAUSTICS

The method of caustics is based on geometric optics and it has been succesfully applied to cases of both transparent and opaque solids. As it is well-known, when speaking about a caustic, we mean a curve or a surface along which a high light-intensity is observed. A *caustic curve* or a *caustic surface* constitutes an envelope of light rays, separating an illuminated from a dark region. In this way, because of the high luminosity of the caustic, this curve (or surface) can clearly be experimentally observed. In what follows, we are concerned only with caustic-curves, which are formed on a reference

screen by intersecting a caustic surface in space. Moreover, although the method of caustics is capable for the experimental determination of various types of stress-fields, where strain-gradients are involved (see references in Theocaris, 1981), attention is focussed in this lecture to the case of cracked bodies.
Referring to an in-plane loading of a specimen, the stress intensification in the region surrounding the crack tip produces a reduction in the thickness of the plate, because of the lateral-contraction effect and/or a variation of the refractive index along the same direction. As a consequence, the incident light rays in the vicinity of the crack tip are deviated and formed the caustic-envelope (Theocaris, 1970;1971). Considering anti-plane loading of a thick cracked plate, the cylindrical curvature formed by the out-of-plane w-displacements acts also as a deflector of light and creates a caustic, which has again the form of a generalized epicycloid (Theocaris, 1979;1981).
Fig. 6 shows a stressed specimen ($S_p$) and a viewing screen (Sc). Points P(x,y), denoted by z=x+iy, on the middle plane of the specimen, have projections P'(X,Y) on the screen, located at a distance $z_o$ from the plate, along the Oz-axis normal to the specimen.

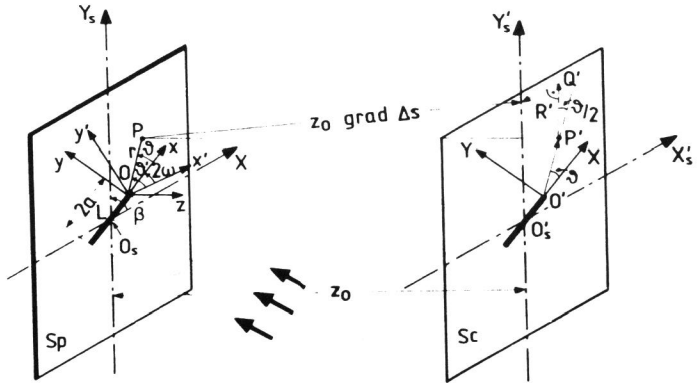


Fig. 6. Geometry of the formation of a caustic from a cracked specimen (Sp) on a screen (Sc).

The mapping of the deflector plate (reflector or refractor) on the screen for a parallel (also convergent, divergent) light beam, impinging normally on the plate, is expressed by

$$\mathbf{W} = \lambda \mathbf{z} + \mathbf{w} \tag{12}$$

where **w** is the complex coordinate of the deviation of the light ray from point P' to point Q, after reflection from, or transmission through, at point P, and $\lambda$ is the magnification factor of the optical apparatus.
Considering that the variation of the refractive index in the vicinity of a crack tip in a transparent plate with parallel lateral faces has the same effect on the passing-through light, as a deformed surface on the incident and reflected light (Theocaris, 1984), we may limit ourselves to the case of reflection from a deformed opaque surface z=f(x,y).
According to *Snellius' law* of reflection, it is valid that

$$\mathbf{w} = w_x \mathbf{i} + w_y \mathbf{j}$$

with

$$w_x = (z-z_0)\tan 2\alpha \quad , \quad w_y = (z-z_0)\tan 2\beta \tag{14}$$

$$\tan\alpha = \frac{\partial f(x,y)}{\partial x} \quad , \quad \tan\beta = \frac{\partial f(x,y)}{\partial y}$$

As a consequence and, by virtue of Eq.(12), the vector **W**=X**i**+Y**j** may be approximated by

$$X = \lambda x - 2z_0 \frac{\partial f(x,y)}{\partial x} \quad , \quad Y = \lambda y - 2z_0 \frac{\partial f(x,y)}{\partial y} \tag{15}$$

where second-order derivatives of the function f(x,y) are neglected, as small when compared to unity, and the f(x,y)-deflection was considered also small, as compared to the distance $z_0$ (far-field optics).
In order to calculate the caustic for a given problem, the function of the deformed surface f(x,y) in Eq.(15), for this problem must be determined. High luminosity of the caustic curve, formed on the screen (either real or virtual), implies that this curve is a singular mathematical curve. That is, for those points on the caustic curve, the mapping (15) is not invertible and the Jacobian of the transformation must vanish, i.e.

$$J(x,y) = \frac{\partial(X(x,y),Y(x,y))}{\partial(x,y)} = 0 \tag{16}$$

The zeroing of the Jacobian is the necessary and sufficient condition for the existence of a caustic curve. The points on the specimen, for which J(x,y)=0, are the points from which the rays forming the caustic are deflected. The locus of these points on the deflecting surface is the so-called *initial curve*. Otherwise, the vanishing of the Jacobian determinant gives the initial curve r=r(ϑ), in polar coordinates, which has the property that every point inside, or outside, this curve maps outside the caustic in the (X,Y)-plane and every point on the initial curve maps on the caustic curve.
As an example consider the topography of the deformed surface around a crack tip under mode-I loading in an isotropic elastic plate indicated in Fig.7, which was initially with parallel lateral faces (Theocaris and Pazis, 1982).

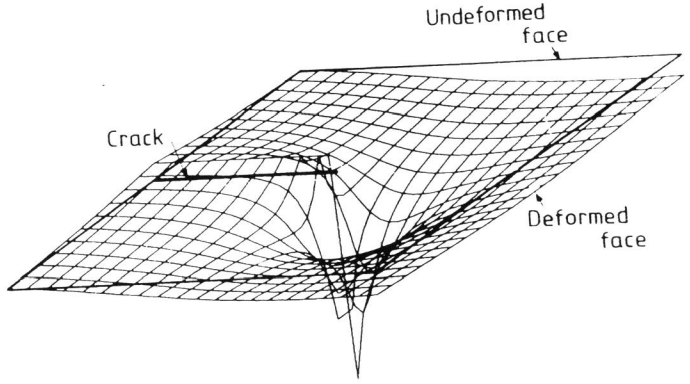


Fig. 7. Topography of the deformed face around a crack tip for mode-I deformation as plotted by computer.

Then, a surface dimple is created in this region of the thin plate under

plane-stress conditions, because of the lateral-contraction effect and the high stress intensity there. Points on the crater, for which the tangent plane has the same slope with respect to the undeformed middle plane of the plate, belong to an initial curve. A large number of initial curves exists, each of which being defined from the parameters of the optical set-up. However, the zone along which these curves can extend is limited to a narrow ring around the crack tip. For the extent of this ring whereundesirable non-linear elastic or plastic strains are occurred near the tip, appropriate values must be given to the optical parameters $\lambda$ and $z_0$. In this case higher-order terms must be also considered in the series-expansion form of stresses, in order to have precise results (Theocaris and Ioakimidis, 1979). It is clear from the above-mentioned general principles of the method that the main cause of deficiencies of all the other optical methods to approach the near-tip region and to take precise measurements from this region disappears in the method of caustics, and this constitutes the basic advantage of the method. Moreover, the experimental arrangements utilized for stationary or dynamic cracks, are very simple and no special care for the specimens is required for tests with caustics. On the contrary, sophisticated arrangements are needed for interferometry and photoelasticity, as well as special preparation for the models in moiré.

We consider now the general case when the rays of a light beam, which impinge on the front surface of a specimen under in-plane deformations, are refracted on this surface, traverse the specimen, are reflected from the rear face of the specimen, traverse once more the specimen and are refracted once more on the front face of it, before they leave the specimen and impinge on the screen. The cases of a single reflection from the front face, when the material is opaque, and the transmission through the specimen without reflection on the rear face of the plate, when transmission optical arrangement is used, are therefore special cases of the general one.
Employing Neumann's strain-optic law (Favre, 1929) and the two-dimensional Hooke's law, either for reflection from the rear face (indicated by the subscript r), or transmission (indicated by the subscript t) we obtain (Theocaris, 1971;1984)

$$\Delta s_{1,2}^{r,t} = dc_{r,t}[(\sigma_{1,2}+\sigma_{2,1}) \pm \xi_{r,t}(\sigma_{1,2}-\sigma_{2,1})] \tag{17}$$

where $c_{r,t}$ denotes the optical constant and $\xi_{r,t}$ the index of optical anistropy.
It is seem from Eq.(17) that, in the general case of optically anisotropic materials, two caustics are formed, each close to the other, since we have two values for the variation of the optical path. Moreover, the shape and the size of these caustics is dependent on the sum, as well as the difference of the principal in-plane stresses.
Although the problem has been also treated for the case of birefringent media (Theocaris and Papadopoulos, 1981), for simplicity in the calculations, we prefer optically isotropic (inert) materials as models. In the latter case $\xi_{r,t}=0$. Thus, only the *first invariant* of the stress tensor influences the characteristics of the respective caustic for a given problem. This is an advantage of the method over the photoelastic method, which is restricted to birefringent models, and its isochromatic patterns depend also on this difference. Moreover, as it has been already mentioned in the analysis of photoelastic method, the difference of the principal stresses is dependent on the radius of the root of any artificial crack or notch, whereas the sum of principal stresses is independent, since the correction terms in the Cartesian components of normal stresses cancel out by addition (Creager and Paris, 1967). Therefore, the geometric characteristics of the caustics, as well as their relationship with the intensity of the fields are not influenced by the geometry of the crack-or notch-tip regions. Consequently, the method can be also applied succesfully to the experimental determination of SIFs in notched plates (Theocaris and Prassianakis, 1980).



In the case of anti-plane (mode-III) deformation of a thick cracked plate the middle plane of the plate is quite free from in-plane stresses and therefore no change of refractive index occurs for the normal- to the lateral-face direction. As a consequence, the classical methods of photoelasticity, interferometry and transmitted caustics are up-to-now incapable to give any information for the evaluation of the intensity of the stress- and displacement-fields around the crack tip.
However, the cylindrical curvature of the lateral faces of the thick plate around the crack tip, induced by the w-displacements, formed a reflected caustic envelope.

The procedure of determining the stress intensity factors, either for in-plane, or out-of-plane crack problems for various cases, treated by Theocaris and his collaborators from the early seventies up-to-now (mechanically isotropic and anisotropic plates, stationary and propagating cracks, static and dynamic loadings, cracked shells, V-notched plates, interfacial cracks, interacting cracks, small-scale yielding in anti-plane shear, Dugdale strip-yield-zone models, birefringent media, etc.) follows the general lines: The parametric equations $X(r,\vartheta)$, $Y(r,\vartheta)$ of the caustic are defined by introducing the respective expression of the deformed surface $f(x,y)$ of the specimen. Usually, these expressions are dependent on the first invariant of the stress tensor and therefore can be derived from Eqs. (2) or (3), or analogous relations. Polar ccordinates are most convenient for the calculations. The zeroing of the Jacobian determinant $\partial(X,Y)/\partial(r,\vartheta)$ gives the initial curve as $r=r(\vartheta)$.
Introduction of this dependence of the polar coordinates to the parametric equations gives the possibility of plotting analytically in a computer, the respective caustic, for various types of loading and material parameters. The latter is not necessary, but by comparing the shapes of the experimentally and analytically generated caustics, one can check the experiment, or the theory. Then, from the equation $\partial Y(\vartheta)/\partial\vartheta=0$, a relation can be established between a geometric characteristic of the caustic (usually the maximum transverse diameter $Y_{max}$) and the stress intensity factor. Thus, with only one measurement of a geometric element of the caustic, formed on a ground-glass reference screen or photographed on this place, and by knowing certain constants of the model tested, one can evaluate accurately the stress intensity factor.
Another advantage of the method of caustics is that no measurement of the crack length is required, contrariwise to all the other optical methods. Such a measurement involves certain difficulties, because the position of the crack tip is not clearly identified.

Experimentally and analytically obtained reflected caustics are illustrated in Figs.8a,8b and 9, for a mode-I, mode-III and mixed-mode cracks, respectively, in an elastic isotropic plate.

Recently, special properties of caustic curves were derived, which are important to applications of fracture mechanics (Theocaris and Pazis, 1981). By using these properties of epicycloids, one can obtain, with a high accuracy, the crack-tip position in the image of the specimen and also can estimate precisely the $K_I$- and $K_{II}$-factors. In Fig. 9, the crack tip may be defined as the section of the lines AA' and BB', which are perpendicular to the pairs of parallel tangents $\varepsilon_1,\varepsilon_1'$ and $\varepsilon_2,\varepsilon_2'$ to the caustic, at a certain position from the tangents.

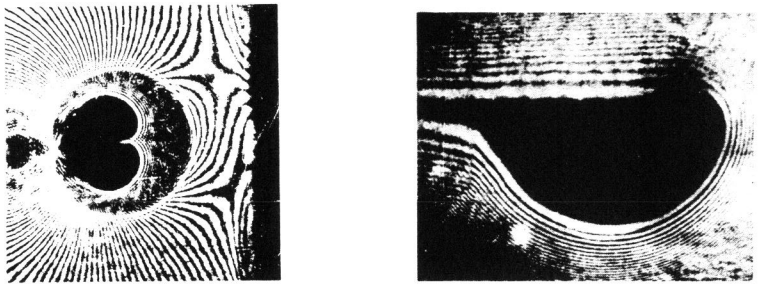

(a) (b)

Fig. 8. Caustics created around tips of a mode-I (a) and mode-III crack (b).

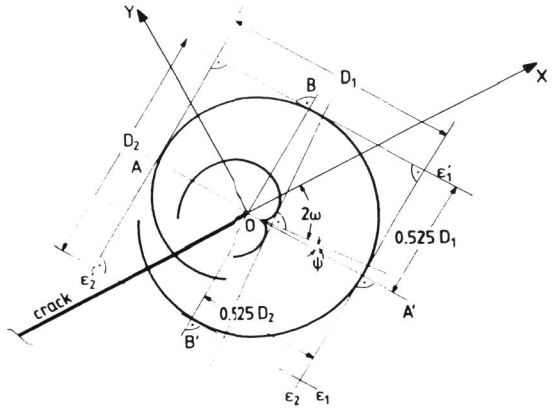


Fig. 9. Analytically obtained mixed-mode caustic and the construction of its center by two pairs of parallel tangents.

Then, the angle $\psi$ can be measured and the respective angle $\vartheta$ on the initial curve, i.e. on the plane of the specimen, is given by

$$\vartheta = \frac{4}{5}\psi \tag{18}$$

The angle $\omega=\arctan(K_{II}/K_I)$ of the inclination of the caustic with the crack axis can be derived from the internal caustic (Theocaris and Joakimides, 1971). If the length $AA'\equiv D(\vartheta)$ defined in Fig.9 is measured, the $K_I$- and $K_{II}$-SIFs may be given by

$$\begin{Bmatrix} K_I \\ K_{II} \end{Bmatrix} = \frac{0.0934}{z_0 dc_r} \frac{1}{\lambda^{3/2}} \left[\frac{D(\vartheta)}{\cos(\vartheta/4+\pi/10)}\right]^{5/2} \begin{Bmatrix} \cos\omega \\ \sin\omega \end{Bmatrix} \tag{19}$$

Fig.10 shows experimentally obtained caustics for a mixed mode crack.

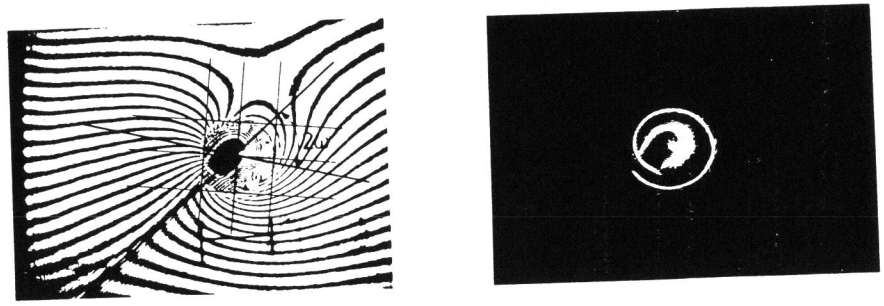


(a) (b)

Fig. 10. Experimentally obtained caustics for a cracked PMMA plate: (a) construction of the center of the rear face caustic from two pairs of parallel tangents and the angle 2ω; (b) reflected rear and front face caustics taken by a divergent laser beam illuminating a very small area around the crack tip.

In the case of mode-I crack propagation in an elastic and brittle plate we have from Eq.( 3 )

$$\sigma_1+\sigma_2 = \frac{K_I B_I}{(2\pi r_1)^{1/2}} 2(\beta_1^2-\beta_2^2)\cos(\vartheta_1/2) \tag{20}$$

Using Eq.(15), the parametric equation of the dynamic caustic may be written in the form

$$X = \lambda x_1 + \varepsilon z_0 dc_j \frac{\vartheta(\sigma_1+\sigma_2)}{\partial x_1}, \quad Y = \lambda y_1 + \varepsilon z_0 dc_j \frac{\vartheta(\sigma_1+\sigma_2)}{\vartheta y_1} \tag{21}$$

where $\varepsilon=1$, $j=f$ for reflected rays from the front face of the specimen, $\varepsilon=1$, $j=t$ for transmitted rays and $\varepsilon=2$, $j=r$ for light rays reflected from the rear face of the specimen, $c_j$ are the optical constants of the material for each case. The correlation of the dynamic SIF, with the maximum transverse diameter of the caustic $D_t^{max}$ is given by the expression

$$K_I = \frac{2(2\pi)^{1/2}}{3\varepsilon z_0 d\lambda^{3/2} c_j} \left(\frac{D_t^{max}}{\delta_{max}}\right)^{5/2} \frac{1}{B_I(\beta_1^2-\beta_2^2)} \tag{22}$$

where $\delta_{max}$ is a *correction factor*, depending only on the crack velocity $\upsilon$ for a given material (Theocaris and Papadopoulos, 1980).
The method of caustic was applied to numerous experimental studies on dynamic fracture by the author in the last six years (see for instance ,Theocaris and Milios, 1980;1981; Theocaris and Georgiadis, 1983;1984).

As a last example of the capabilities of the method to yield results in complicated stress fields, we consider the case of a branched running crack of Fig.11 (Theocaris and Pazis, 1983).

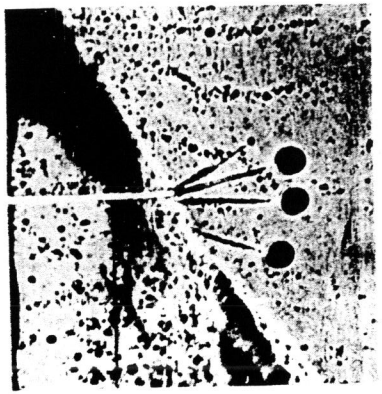

Fig. 11 . Photograph of a dynamic crack splitted in four branches after the passing of an inclined interphase.

In this experiment, after the propagating crack has passed through a slant interphase, it was splitted in four branches. Equal in number caustics are appeared in the photographs of the high-speed camera, which yield the intensities of the respective stress fields. A comparison between Figs. 4 and 11, which illustrate bifurcated cracks, shows clearly another advantage of the caustic method over the photoelastic method.

Finally, the inherent accuracy of the method should be pointed out. The caustics can be adjusted to correspond to an infinitesimal region (and regulable) around the crack tip, where the elastic-stress singularity completely dominates the stress field, whereas there is no deleterious influence of non-linear effect of the core region. All other methods need to make measurements outside this region for obtaining, first readable, and then reliable data. This fact is well presented in the perfect hologram shown in Fig. 3 , by Dudderar and O'Regan (1971), where they mention that their accidentally obtained caustic, formed in the close vicinity of a crack tip, is considered as a region excluded from measurements. However, only the method of caustics is capable to provide information in this region, which is of much interest in fracture mechanics. Thus, the method may be considered at least of one-order higher accuracy, than any other experimental method and therefore is almost independent of higher-term approximations introduced recently in the literature (Theocaris and Spyropoulos, 1982;1983; Rossmanith, 1980).

Finally, in problems of bending of plates and shells and all other cases, where out-of-plane loadings are applied in cracked bodies, all other experimental methods fail up-to-now to give satisfactory results, whereas the method of reflected caustics has been extended with great success (Theocaris, 1979; 1982).

ACKNOWLEDGEMENT

The author gratefully acknowledges the assistance of his Research Associate Mr. H.G. Georgiadis during the preparation of the paper.



REFERENCES

Betser, A.A., A.S. Kobayashi, O.S. Lee and B.S.J. Kang (1982). Crack-tip dynamic isochromatics in the presence of small-scale yielding. *Exp. Mech.*, **22**, 132-138.

Born, N. and E. Wolf (1970). Principles of optics. *Pergamon Press.*

Bradley, W.B. and A.S. Kobayashi (1970). An investigation of propagating cracks by dynamic photoelasticity. *Exp. Mech.*, **10**(3), 106-113.

Bradley, W.B. and A.S. Kobayashi (1971). Fracture dynamics-A photoelastic investigation. *Engng. Fract. Mech.*, **3**, 317-332.

Cartwright, D.J. and E.P. Rooke (1974). Approximate stress intensity factors compounded from known solutions. *Engng. Fract. Mech.*, **6**, 563-590.

Creager, M., and P.C. Paris (1967). Elastic field equations for blunt cracks with reference to stress corrosion cracking. *Int. J. Fract.*, **3**, 247-252.

Dally, J.W. and T. Kobayashi (1978). Crack arrest in duplex specimens. *Int. J. Solids Structures*, 14, 121-129.

Dally, J.W. (1979). Dynamic photoelastic studies of fracture. *Exp. Mech.*, 349-361.

Dudderar, T.D. and R.O'Regan (1971). Measurement of the strain field near a crack tip in polymethylmethacrylate by holographic interferometry. *Exp. Mech.*, **28**(1), 49-56.

Durelli, A.J. and V.J. Parks (1970). Moiré analysis of strain. *Prentice-Hall*, Englewood Cliffs, NJ.

Etheridge, J.M. and J.W. Dally (1977). A critical review of methods for determining stress-intensity factors from isochromatic fringes. *Exp. Mech.*, **17**, 248-254.

Etheridge, J.M. and J.W. Dally (1978). A three-parameter method for determining stress intensity factors from isochromatic fringe loops. *J. Strain Anal.*, **13**, 91-94.

Favre, H. (1929). Sur une nouvelle méthode optique de determination des tensions intérieures. *Revue Opt.*, **8**, 193-213, 241-261, 289-307.

Fourney, M.E. (1968). Application of holography to photoelasticity. *Exp. Mech.*, **25**(1), 33-38.

Gabor, D. (1948). A new microscopic principle. *Nature*, **161**, 777-778.

Hartranft, R.J. and G.C. Sih (1968). Effect of plate thickness on the bending stress distribution around through cracks. *J. Math. Phys.*, **47**(3), 276-291.

Hartranft, R.J. and G.C. Sih (1970). An approximate three-dimensional theory of plates with application to crack problems. *Int. J. Engng. Sci.*, **8**, 711-729.

Holloway, D.C. et al. (1978). Dynamic fracture-toughness determination from isopachics of a running crack. *SESA Fall Meeting*, Munich.

Hutchinson, J.W. (1968). Plastic stress and strain fields at a crack tip. *Int. J. Mech. Phys. of Solids*, **16**, 337-347.

Ioakimidis, N.I. and P.S. Theocaris (1978). A simple method for the photoelastic determination of mode-I stress intensity factors. *Engng. Fract. Mech.*, **10**, 677-684.

Irwin, G.R. (1957). Analysis of stresses and strains near the end of a crack traversing a plate. *J. Appl. Mech., Trans. ASME*, **79E**, 361-364.

Irwin, G.R. (1958). Fracture. *Handbuch der Physik*, **6**, 551-590.

Irwin, G.R. (1958). Discussion. *Proc. SESA*, **16**(1), 93-96.

Irwin, G.R. et al. (1979). On the determination of the a-k relationship for birefringent polymers. *Exp. Mech.*, **19**(4), 121-128.

Kanninen, M.F. (1968). An estimate of the limiting speed of a propagating ductile crack. *J. Mech. Phys. Solids*, 16, 215-225.

Kobayashi, A.S., W.B. Bradley and R.A. Selby (1965). Transient analysis in a fracturing epoxy plate. *Proc. of the 1st Int. Conf. Fract.*, 3, 1809-1831.

Kobayashi, A.S., D.O. Harris and W.L. Engstrom (1967). Transient analysis in a fracturing magnesium plate. *Exp. Mech.*, **7**(10), 434-440.

Kobayashi, A.S., W.L. Engstrom and B.R. Simon (1969). Crack opening displacements and normal strains in centrally notched plates. *Exp. Mech.*, **9**(4), 163-170.

Kobayashi, A.S., A.F. Emery and S. Mall (1977). Dynamic finite element and dynamic photoelastic analysis of crack arrest in Homalite-100 plates. *Fast Fracture and Crack Arrest*, ASTM STP **627**, 95-108.

Kobayashi, A.S. and M. Ramulu (1981). Dynamic stress-intensity factors for unsymmetric dynamic isochromatics. *Exp. Mech.*, **21**(1), 41-48.

Kobayashi, T. and J.W. Dally (1977). The relation between crack velocity and the stress intensity factor in birefringent polymers. *Fast Fracture and Crack Arrest*, ASTM STP 627, 257-273.

Kolosoff, G. (1909). Doctoral dissertation.

Leith, E.N. and J. Upatnieks (1963). Wavefront reconstruction with continuous tone objects. *Jnl. Opt. Soc. America*, **52**, 1123; **53**, 1377.

Leith, E.N. and J. Upatnieks (1964). Wavefront reconstruction with diffused illumination and three-dimensional objects. *Jnl. Opt. Soc. America*, **54**, 1295.

Liebowitz, H., J. Lee and J. Eftis (1978). Biaxial load effects in fracture mechanics. *Engng. Fract. Mech.*, **10**, 315-335.

Mall, S., A.S. Kobayashi and Y. Urabe (1978). Dynamic photoelastic and dynamic finite element analyses of dynamic-tear-test specimens. *Exp. Mech.*, **18**(12), 449-456.

Muskhelishvili, N.I. (1953). Some basic problems of the mathematical theory of elasticity. Noordhoff Publ.

Oppel, G.V. and P.W. Hill (1964). Strain measurements at the root of cracks and notches. *Exp. Mech.*, 4(7), 206-211.

Paris, P.C. and G.C. Sih (1965). Stress analysis of cracks. ASTM STP 381, 39-76.

Post, D. (1953). Photoelastic stress analysis for an edge crack in a tensile field. *Proc. SESA*, **12**(1), 99-116.

Radok, J.R.M. (1956). On the solution of problems of dynamic plane elasticity. *Quart. Appl. Math.*, **14**, 289-298.

Rayleigh, Lord (1874). On the manufacture and theory of diffraction gratings. *Phil. Mag.*, **47**(310), 81-93, **47**(311), 193-205.

Riley, W.F. and J.W. Dally (1969). Recording dynamic fringe patterns with a Cranz-Schardin camera. *Exp. Mech.*, **9**(8), 27N-33N.

Rossmanith, H.P. and G.R. Irwin (1979). Analysis of dynamic isochromatic crack-tip stress patterns. *University of Maryland Report.*

Rossmanith, H.P. (1979). Dynamic stress-intensity-factor determination from isopachics. *Exp. Mech.*, 19, 281-285.

Rossmanith, H.P. (1980). The method of caustics for mixed-mode crack loading with higher order term effects. *Engng. Fract. Mech.*, **13**, 991-1000.

Schroedl, M.A., J.J. McGowan and C.W. Smith (1972). An assessment of factors influencing data obtained by the photoelastic stress freezing technique for stress fields near crack tips. *Engng. Fract. Mech.*, **4**, 801-809.

Schroedl, M.A., J.J. McGowan and C.W. Smith (1974). Determination of stress-intensity factors from photoelastic data with applications to surface-flaw problems. *Exp. Mech.*, **14**(10), 392-399.

Sih, G.C., P.C. Paris and F. Erdogan (1962). Crack-tip, stress-intensity factors for plane extension and plate bending problems. *J. Appl. Mech., Trans. ASME*, **84E**, 306-312.

Sih, G.C., P.C. Paris and G.R. Irwin (1965). On cracks in rectilinearly anisotropic bodies. *Int. J. Fract.*, **1**, 189-203.

Sih, G.C. (1973). Handbook of stress intensity factors for researchers and engineers. *Inst. Fract. Sol. Mech.*, Lehigh Univ., Bethlehem, PA.

Smith, C.W. (1975). Use of three-dimensional photoelasticity and progress in related areas. *Exp. Techn. in Fract. Mech.*, ed. A.S. Kobayashi, 2, 3-20.

Smith, C.W. (1981). Use of photoelasticity in fracture mechanics. *Experimental evaluation of stress concentration and intensity factors*, ed. G.S. Sih, Nijhoff Publ. 163-187.

Tada, H., P.C. Paris and G.R. Irwin (1973). The stress analysis of cracks handbook. *Del. Research Corp.*, Hillertown, PA.

Theocaris, P.S. (1963). Diffused light interferometry for measurement of isopachics. *J. Mech. Phys. of Solids*, **11**(3), 181-195.

Theocaris, P.S. (1969). Moiré fringes in strain analysis. *Pergamon Press*, Oxford.

Theocaris, P.S. (1970). Local yielding around a crack tip in plexiglas. *J. Appl. Mech.*, **37**, 409-415.

Theocaris, P.S. (1971). Reflected shadow method for the study of constrained zones in cracked plates. *Appl. Optics*, **10**, 2240-2247.

Theocaris, P.S. (1971). On a geometric interpretation of holography. *Technical Annals* (in Greek with English summary), 861-868.

Theocaris, P.S. (1979). Antiplane shear stress intensity factor evaluated by caustics. *Proc. Nat. Academy Athens* (in English with Greek Summary), **54**(3), 368-383.

Theocaris, P.S. (1979). Symmetric bending of cracked plates studied by caustics. *Int. J. Mech. Sci.*, **21**, 659-670.

Theocaris, P.S. (1981). The reflected caustic method for the evaluation of mode III stress intensity factors. *Int. J. Mech. Sci.*, **23**, 105-117.

Theocaris, P.S. (1982). Complex stress intensity factors in bent plates with cracks. *J. Appl. Mech.*, **49**, 87-96.

Theocaris, P.S. (1984). Caustics in plane strain-Evaluation of COD and the core region. *Engng. Fract. Mech.*, **19**(1), 81-92.

Theocaris, P.S. and E.E. Gdoutos (1977). Comments on a paper entitled: Limitations of the Westergaard equations for experimental evaluation of stress intensity factors, by W.T. Evans and A.R. Luxmoore, *J. Strain Anal.*, **12**, 349-350.

Theocaris, P.S. and E.E. Gdoutos (1978). A photoelastic determination of $K_I$ stress intensity factor. *Engng. Fract. Mech.*, **7**, 331-339.

Theocaris, P.S. and H.G. Georgiadis (1983). Dynamic interaction of a propagating crack with an oblique fault. *Int. J. Soil Dyn. Earth. Engng.*, **2**(3), 161-170.

Theocaris, P.S. and H.G. Georgiadis (1984). Crack propagation in layered plates - An experimental study, *Exp. Mech.* (submitted for publication).

Theocaris, P.S. and N.I. Ioakimidis (1979). An improved method for the determination of mode I stress intensity factors by the experimental method of caustics. *J. Strain Anal.*, 14, 111-118.

Theocaris, P.S. and N. Joakimides (1971). Some properties of generalized epicycloids applied to fracture mechanics. *Zeits. für ang. Math. Phys.*, **22**, 876-890.

Theocaris, P.S. and J. Milios (1980). Dynamic crack propagation in Composites. *Int. J. Fracture*, **16**, 31-51.

Theocaris, P.S. and J. Milios (1981). Crack-arrest at a bimaterial interface. *Int. J. Solids Structures*, 17, 217-223.

Theocaris, P.S. and G.A. Papadopoulos (1980). Elastodynamic forms of caustics for running cracks under constant velocity. *Engng. Fract. Mech.*, **13**, 683-698.

Theocaris, P.S. and G.A. Papadopoulos (1981). Stress intensity factors from reflected caustics in birefringent plates with cracks. *J. Strain Anal.*, **16**, 29-36.

Theocaris, P.S. and D. Pazis (1981). Some further properties of caustics useful in mechanical applications. *Appl. Optics*, **20**, 4009-4018.

Theocaris, P.S. and D. Pazis (1983). The topography of the core-region around cracks under modes I,II and III of fracture. *Int. J. Mech. Sci.*, **25**(2), 121-136.

Theocaris, P.S. and D. Pazis (1983). Crack deceleration and arrest phenomena at an oblique bimaterial interface. *Int. J. Solids Structures*, **19**(7), 611-623.

Theocaris, P.S. and D. Prassianakis (1980). Stress intensity factors in elastic plates with re-entrant corners asymmetrically loaded. *J. Strain Anal.*, **15**(4), 195-200.

Theocaris, P.S. and C.P. Spyropoulos (1982). An optimization process for evaluating complex stress intensity factors in cracked plates from isopachics. *Materialprüf.*, **24**(11), 402-406.

Theocaris, P.S. and C.P. Spyropoulos (1983). Photoelastic determination of complex stress intensity factors for slant cracks under biaxial loading with higher-order effects. *Act. Mech.*, **48**, 57-70.

Villarreal, G. and G.C. Sih (1981). Three-dimensional photoelasticity: stress distribution around a through thickness crack. *Experimental evaluation of stress concentration and intensity factors*, ed. G.S. Sih, Nijhoff Publ., 253-280.

Wells, A. and D. Post (1958). The dynamic stress distribution surrounding a running crack-A photoelastic analysis. *Proc. SESA*, **16**(1), 69-92.

Yoffé, E.H. (1951). The moving Griffith crack. *Phil. Mag.*, **42**, 739-750.